WARSAW UNIVERSITY OF TECHNOLOGY Index 351733
FACULTY OF CIVIL ENGINEERING
COMMITTEE FOR CIVIL AND WATER ENGINEERING
POLISH ACADEMY OF SCIENCES ISSN 1230-2945
DOI: 10.24425/ace.2024.149874
ARCHIVES OF CIVIL ENGINEERING
Vol. LXX ISSUE 2 2024
pp. 447 –460

Research paper

Structural optimization design of multi ribbed composite wall of building components under seismic load based on random optimization algorithm and resilience model

Xu Hu[1], Lu He[2]

Abstract: The multi ribbed composite wall structure is also known as the multi ribbed wall panel light frame structure. This structure is suitable for housing construction in the residential field. The special structural failure process and mode of multi ribbed composite walls are different from traditional walls. To fully utilize the excellent structural performance in building construction and improve the seismic performance of the building, based on the transformation principle of subset optimization algorithm for optimization problems, a constrained subset simulation optimization algorithm suitable for optimizing the maximum displacement angle of multi ribbed composite wall panels is designed. The Bayesian algorithm is used to construct a restoring force model for multi ribbed composite wall panels. The constrained subset simulation optimization algorithm and resilience model are used to optimize the seismic performance of 4-layer multi ribbed composite wall panels. The results show that the section height and the equivalent slant support width of the continuous column for the 4-story multi ribbed composite wall panel change from discrete distribution to aggregation with the increase of iteration. Finally, the sampling is stable in the 9th floor. At this time, the section height of the continuous column is 230 mm, and the equivalent slant support width is 525. After optimization, the failure probability of both extreme displacement angle states has decreased. When the peak ground acceleration is 1.0 g, the optimized second limit state failure probability is less than 100%. When the peak ground acceleration value is between 0.2 g and 0.6 g, both limit states show a rapid upward trend. The constrained subset simulation optimization algorithm and Bayesian quantitative resilience model proposed in the research can effectively optimize the seismic performance of multi ribbed composite walls.

Keywords: multi-ribbed composite wall, random optimization, resilience model, SSO, structural optimization

[1]MSc., Department of Real Estate and Engineering Management, Liaoning Urban Construction Technical College, Shenyang, 110122, China, e-mail: 15541568826@163.com, ORCID: 0009-0005-7348-9761
[2]MSc., Department of Real Estate and Engineering Management, Liaoning Urban Construction Technical College, Shenyang, 110122, China, e-mail: Helu0248879@163.com, ORCID: 0009-0004-8571-4789

1. Introduction

With the development of modern industrial technology, the structural system of building construction is also increasing. The multi-ribbed composite wall (MRCW) structure, also known as the multi-ribbed wall panel light frame structure, is commonly used in the construction of residential buildings [1, 2]. The failure mode of MRCW structure is influenced by the ratio of wall panels and frames, the strength of filled blocks, and the elastic modulus. The parameters of MRCW include integer variables and continuous variables. The optimization design methods for traditional building components have limited effectiveness. Therefore, for the MRCW structure, a reasonable improvement algorithm needs to be designed for structural optimization [3]. The optimization problem of MRCW structure and the solution of restoring force model parameters both require rich stress analysis and calculation. The data is large in scale and highly non-linear. However, traditional numerical optimization algorithms have low computational efficiency [4]. It is prone to falling into the dilemma of local optimal solutions. The global optimization ability of random optimization algorithms is effective, which has efficient computational efficiency, making them suitable for solving high data scale problems. Based on this, random optimization algorithms and resilience models are used to optimize the MRCW structures in building components. It is expected to fully utilize the excellent structural performance in building construction and improve the enhance performance.

2. Related works

There is sufficient research on wall components and construction in architecture. MRCWs, as the main load-bearing components of building structures, have also received much attention. Sun et al. explored the temperature and residual bearing capacity of the filled frame of the MRCW structure after high temperature through experiments and finite element analysis. The axial compression test is used to evaluate the mechanical properties of MC at high temperatures. The finite element (FE) model of the infill frame under oblique loads is developed. The relationship between residual bearing capacity and fire exposure time is obtained [5]. Ismail et al. focused on improper evaluation and information management of thermal comfort in prefabricated concrete buildings. The feasibility and benefits of using ICT for new solutions in PC building projects where natural ventilation levels are inconsistent with occupant comfort are analyzed. The results indicate that this solution is crucial for optimizing the thermal comfort and energy efficiency of PC building projects [6]. Han et al. focused on the incorrect installation and operation of heavy lifting equipment in structured building construction. The visualization design of hoisting based on dynamic three-dimensional trajectory is used in a data-driven crane management system. The results indicate that it can reduce lifting time, improve safety and quality [7].

There are abundant intelligent optimization algorithms suitable for solving optimization strategy problems. Among them, random optimization algorithms have been applied in various fields. Li et al. proposed a novel topology optimization framework based on SS

by combining subset simulation (SS) with generative adversarial networks (GAN). The topology optimization (TO) algorithm guided by SS and GAN can promote efficient TO of periodic structures. The effectiveness and efficiency of the method are demonstrated through TO of two-dimensional periodic structures [8]. Ezaleden et al. used the NPSO algorithm to learn the importance of relationship types between concepts. A simulated recommendation system based on the highest ranking for dynamic learners is constructed. The CLM and ECLM conceptual models are learned. The simulation results demonstrate that the performance of ECLM is better than other existing methods, with an average Interchange Rating (MRR) value of 0.780 [9].

In summary, scholars have focused on the bearing capacity and safety issues of buildings and conducted extensive research on composite wall frame structures. However, there is still limited research on the structural performance of MRCWs. The performance advantages of MRCW structures in terms of earthquake resistance and support cannot be fully explained. MRCWs have high seismic application value. The structure is complex. How to fully utilize the potential application value of the performance advantages has become a research focus.

3. Optimization design of multi-ribbed composite wallboard based on SSO algorithm and resilience model

To design a random optimization algorithm and restoring force model suitable for optimizing the seismic performance of MRCW panels, a subset simulation optimization algorithm is first optimized based on the structural features of the MRCW panel, making it to optimize constrained problems. On the other hand, Bayesian theory is used to construct a restoring force model, which can be used for simulating the maximum displacement angle parameters of multi-ribbed composite wall panels.

3.1. Problem-solving solution based on SSO algorithm

The algorithm foundation of the research is the Subset Simulation Optimization (SSO) algorithm. The basic idea of the SSO algorithm is to construct the problem to be optimized into a reliability analysis problem [10, 11]. By introducing probability assumptions into the design variables, artificial randomness is added to the objective problem function. Taking the maximum value of the objective function for solving a multi-parameter problem as an example, the conditional formula for the function solution is shown in Eq. (3.1).

$$g_{\text{opt}} = g(x_{\text{opt}}) \geq g(x) \ \forall x \in \Omega \tag{3.1}$$

In Eq. (3.1), Ω represents the set of design variable spaces, $\Omega \in R^n$, g_{opt} is the global maximum. The solution of the corresponding design variable is x_{opt}. The target failure event occurrence conditions for the reliability analysis problem of SSO construction are shown in Eq. (3.2).

$$F = \{g(x) \geq b\} \tag{3.2}$$

In Eq. (3.2), F is the target failure event. b is the threshold at which the small failure event occurs. The critical value of the structural response is taken as this value. Intermediate events are introduced to transform small failure probability events into a series of conditional probability event products with high occurrence probability. When the intermediate event satisfies a nested relationship, $F_1 \supset F_2 \supset \ldots \supset F_m = F$. The probability expression is shown in Eq. (3.3).

$$P_F = P(F) = P(F_m) = P(F_m|F_{m-1})P(F_{m-1}) = \ldots = P(F_1)\prod_{i=2}^{m} P(F_i|F_{i-1}) \tag{3.3}$$

In Eq. (3.3), m represents the intermediate events. The conditional probability of intermediate events is $P(F_i|F_{i-1})$. When the value is large, the efficiency of simulation P_F is higher, which can improve the efficiency of simulation operations. The expression for intermediate events is shown in Eq. (3.4).

$$F_i = \{g(s) \geq b_{i-1}, i = 2, \ldots, m\} \quad (b_1 < b_2 < \ldots < b_m = b) \tag{3.4}$$

The failure domain of reliability calculation includes the target variable value of optimization calculation. Therefore, optimization problems can be solved within the framework of reliability. Since reliability analysis is a probability analysis, the design variables for optimization analysis within the framework need to be "randomized". Therefore, the target variable has randomness [12, 13]. The design variable solution corresponding to the maximum of the target function is $x = x_{\text{opt}}$. The expression for converting into a reliability problem is shown in Eq. (3.5).

$$p_g = P(g) = P(g(x) \geq g_{\text{opt}}) \tag{3.5}$$

In Eq. (3.5), the probability of failure event $F_g = \{g(x) \geq g_{\text{opt}}\}$ occurring is 0. The mathematical model of constrained optimization problems is shown in Eq. (3.6).

$$\begin{aligned} &\max\ W(x) \\ &s.t. \begin{cases} g_i(x) = g_i(x_1, x_2, ..., x_n) \leq 0 & (i = 1, 2, ..., l) \\ h_j(x) = h_j(x_1, x_2, ..., x_n) = 0 & (j = 1, 2, ..., k) \end{cases} \quad x \in S \end{aligned} \tag{3.6}$$

In Eq. (3.6), the objective function is represented as $W(x)$. The i-th inequality constraint is represented as$g_i(x)$. l represents the total number of inequality constraints. The constraint condition of the j-th equation is expressed as $h_j(x)$. k represents the total number of equality constraints. S is the problem search domain. By defining global constraint functions, constraint conditions are integrated. For inequality constraints, for inequality constraints, the violation function is shown in Eq. (3.7).

$$v_i(x) = \begin{cases} 0, & g_i(x) \leq 0 \\ g_i(x), & g_i(x) > 0 \end{cases} \tag{3.7}$$

According to the definition of inequality constraint violation function, the violation function of equality constraint condition is shown in Eq. (3.8).

$$v_j(x) = \left|h_j(x)\right| \geq 0 \tag{3.8}$$

The inequality constraint violation function and the equality constraint violation function are integrated to define the global constraint function, as shown in Eq. (3.9).

$$F_{\text{con}}(x) = -\max v_i \tag{3.9}$$

In Eq. (3.9), v_i denote the set of inequality constraint violation functions and equation constraint violation functions, and only when the variable is in the feasible region of the constraint condition, $F_{\text{con}}(x) = 0$. All solutions in this domain satisfy $F_{\text{con}}(x) = 0$.

3.2. Optimization scheme for seismic performance of MRCW panels based on SSO

Due to the constraint conditions, during optimization, samples that meet the constraint conditions are selected from the current sample set. Then the next stage of optimization is entered. Afterwards, the global constraint function is used as the first sorting criterion. The feasibility of the objective function is used as the second sorting criterion to sort the samples. The algorithm flowchart is shown in Fig. 1.

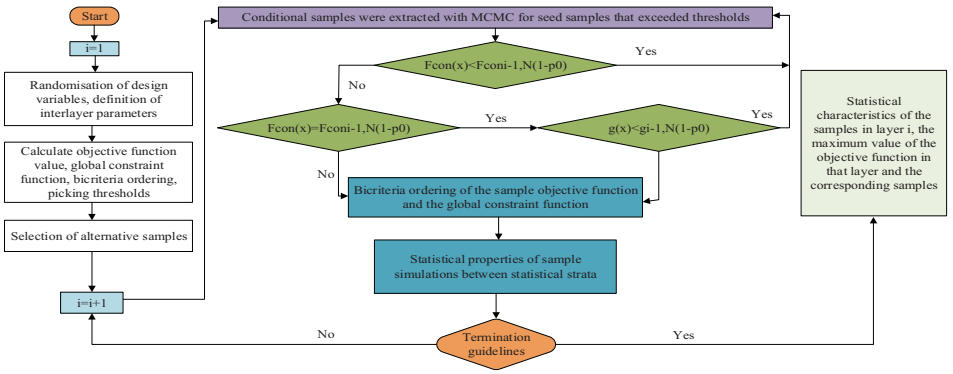

Fig. 1. SSO algorithm flowchart

In Fig. 1, The Markov chain Monte Carlo (MCMC) algorithm is applied to extract generating conditional samples. After sorting the sample objective function and global constraint function in a dual standard order, the statistical characteristics of the inter layer simulated samples are calculated. The incremental dynamic analysis (IDA) method is used to analyze the vulnerability of MRCW structures [14]. In the vulnerability analysis of MRCW structures, Peak Ground Acceleration (PGA) is taken as *IM*. The maximum displacement angle (DA) between floors is taken as *DM*. The calculation process is shown in Eq. (3.10).

$$\hat{D} = a \cdot IM^b \tag{3.10}$$

Firstly, as shown in Eq. (3.10), $\hat{D}$ represents the median value of earthquake demand, which follows a normal distribution. By taking logarithms on both sides of the equation, the earthquake probability demand model can be obtained as shown in Eq. (3.11).

$$\ln \hat{D} = \ln a + b \cdot \ln IM \tag{3.11}$$

The data obtained by IDA can be regressed in the logarithmic distribution space to obtain ln *a* and *b*.

After analyzing the seismic performance, the seismic performance is optimized by optimizing the maximum interlayer displacement angle under earthquake action. The specific steps are shown in Fig. 2.

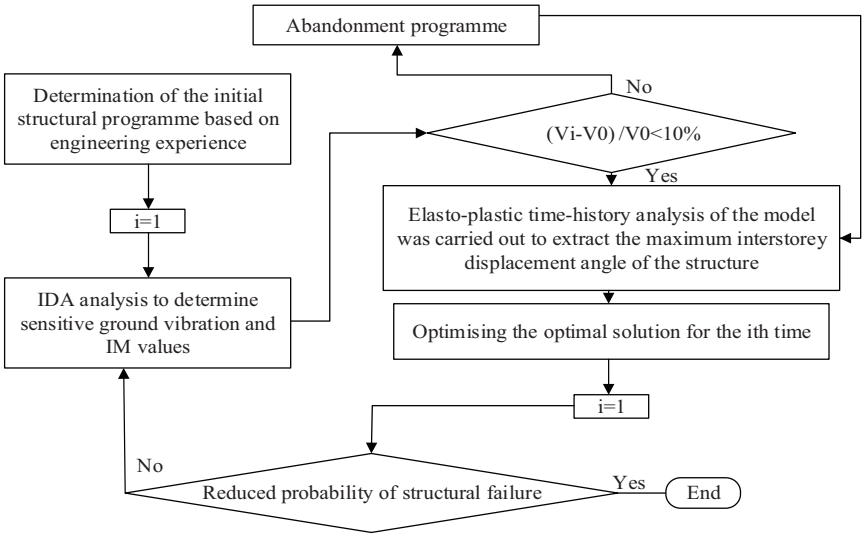

Fig. 2. Specific steps for optimizing seismic performance with maximum inter story displacement angle

Firstly, based on consulting design data and on-site engineering research, the parameters of the wall structure are determined. The IDA is applied for vulnerability analysis, seismic motion, and *IM* values. Afterwards, the constrained SSO algorithm is used to generate an optimized design scheme through sampling. If the structure meets the requirements of the standard design and meets the constraints, modifications will be made according to the optimized design plan. The alternative *IM* value is used for elastic-plastic time history analysis. The scheme to minimize the maximum DA between floors is determined. Afterwards, the existing optimal solution is subjected to IDA analysis to determine whether the probability of structural failure has decreased [15].

3.3. Construction scheme of restoring force model for MRCW structure

The RFM is a mathematical model that reflects the relationship between the restoring force of a structure or component and its deformation, which is the basis for conducting nonlinear structural analysis. The restoring force model of the MRCW panel and the RFM of the component section are constructed. The RFM of the component section is constructed using Fiber Section (FS), as shown in Fig. 3.

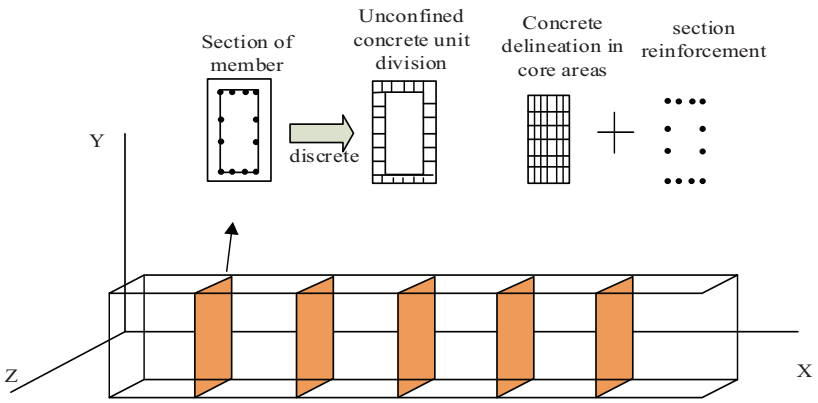

Fig. 3. Fiber cross section

FS can divide beam and column components into discrete elements represented by the stress-strain relationship of the corresponding material. The cross-section is smooth. The bending moment-curvature relationship of the component section is less affected by shear stress. Therefore, the effect of shear force can be ignored when deriving the relationship between bending moment-curvature. When calculating the stress and strain of components, the changes caused by factors such as temperature, time, and humidity are ignored. The influence of bond slip for steel bars is not considered. The degenerate bilinear restoring force model is selected to simulate the restoring force model of a 4-floor MRCW plate structure, as displayed in Fig. 4.

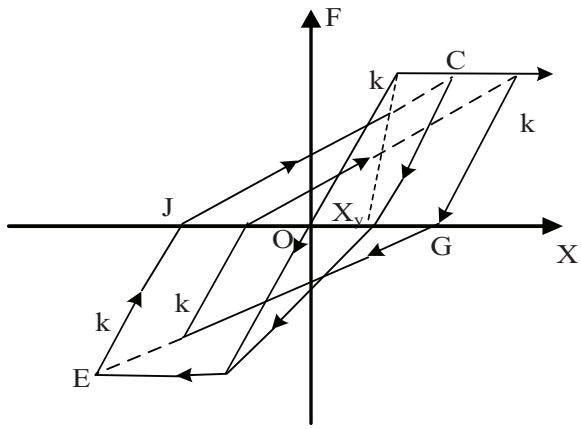

Fig. 4. Interlayer restoring force model of 4-layer multi ribbed composite plate structure

The eigenvalues of the degenerate bilinear model include elastic stiffness k, yield stiffness k', and yield displacement x_y. Therefore, the parameters to be identified are set as follows. The elastic stiffness are k_1, k_2, k_3, and k_4 respectively. The yield stiffness are

k_1', k_2', k_3', and k_4'. The yield displacements are X_{y1}, X_{y2}, X_{y3}, and X_{y4}, with a total of 12 parameters. Bayesian method is used to construct resilience models. Based on Bayesian theory and measured data, the posterior distribution of the target parameter variable is calculated, as shown in Eq. (3.12).

(3.12)

$$p(Y(t)|\theta) = \exp(L(\theta)) = \left(\prod_{i=1}^{R} \frac{1}{(\sqrt{2\pi}\sigma_i)^{N_i}}\right) \exp\left\{\sum_{i=1}^{R}\sum_{j=1}^{N_j} -\frac{1}{2\sigma_i^2}\left[y_i(j) - x_i(\theta, j)\right]^2\right\}$$

4. Example analysis of optimization schemes for MRCW panels seismic performance

4.1. Seismic response analysis of dense ribbed composite wall panel model

Based on the proposed optimization design scheme for seismic performance of MRCW panels, a case study is conducted on a 4-story MRCW panel to verify the effectiveness of the proposed scheme. The construction of 4-layer dense-ribbed composite wall panel is based on the Code for Seismic Design of Buildings (GB50011-2010), Technical Specification for Dense-Ribbed Composite Panel Structure (JCJ/T 275-2013) and the actual project information, which sets the structural storey height of 3.3 m, the wall thickness of 200 mm, and the dimensions of the frame columns and concealed beams of 200 × 200 mm and 200 × 300 mm, respectively. Referring to the specification of a 4-layer dense ribbed composite wall panel and (JCJ/T 275-2013), the wall concrete selects C25, wall panel beams and columns concrete selects C20, and autoclaved aerated concrete is used to fill in the wall, and the three-dimensional three-dimensional diagram and the plan layout diagram are shown in Fig. 5.

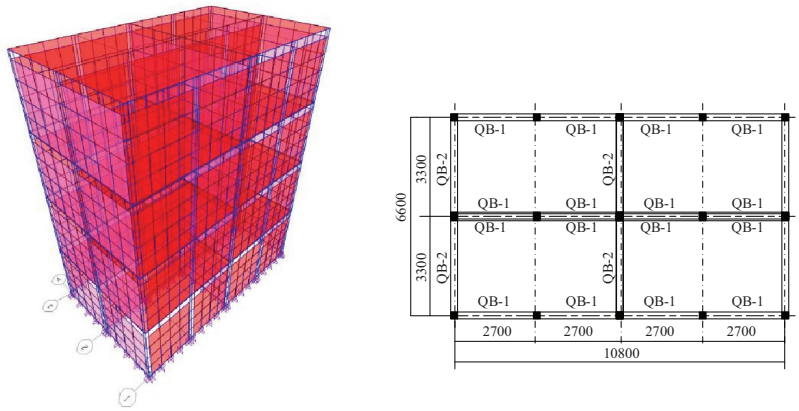

Fig. 5. 3D structure and layout plan: a) Three-dimensional figure, b) Layout plan

In Fig. 5, the seismic fortification intensity is 8. The live load is 0.5 kN/m^2. The dead load is 7.0 kN/m^2. OpenSees is used to establish finite element models. Beam, column and equivalent slant support components are taken as basic elements. Table 1 displays the parameters.

Table 1. Model parameters

Wall panel number	**Eaq (N/mm^2)**		**Width of slant support (mm)**		**Weightiness (N/mm)**
QB-1	7016.67		437.63		2.48×10^{-5}
QB-2	6492.47		480.75		2.41×10^{-5}
Equivalent slant support and concrete constitutive parameters					
–	Peak pressure (N/mm^2)	Peak strain	Ultimate stress (N/mm^2)	Ultimate strain	Elastic modulus (GPa)
QB-1	10.523	0.003	2.105	0.006	7.017
QB-2	9.838	0.003	1.948	0.006	6.492
C25 unconstrained concrete	–24.235	0.0015	0	0.004	31.68
C25 core area concrete	–29.082	0.0018	–6.98	0.018	
C30 unconstrained concrete	–28.03	0.0017	0	0.004	33.01
C30 core area concrete	–33.64	0.002	–8.07	0.02	

The elastic modulus of the 4-layer ribbed composite wall panel filled with autoclaved aerated concrete block is 1600 N/mm^2. The weight is $5.5 \cdot 10^{-6}$ N/mm^3. The elastic modulus of C20 concrete is $2.55 \cdot 10^4$ N/mm^2. The weight is $2.5 \cdot 10^{-5}$ N/mm^3. Through comprehensive calculation, the equivalent elastic modulus, equivalent width and equivalent weight of equivalent slant support of 4-layer MRCW panel can be obtained. The results are shown in Table 1. According to the Code for Design of Concrete Structures (GB50010-2010), various parameters of concrete can be calculated. The above parameters are used for OpenSees modeling and vulnerability analysis. The results are shown in Fig. 6.

In Fig. 6, at the natural vibration period $T = 0.29$ s of the 4-layer MRCW plate structure, the design response spectrum of the structure corresponds to an acceleration value of 0.9 g. The average response spectrum corresponds to an acceleration value of 0.95 g, with an error of 5.6%. It indicates that the error between the mean response spectrum and the design response spectrum at their natural vibration period is small. The selected wave is reasonable.

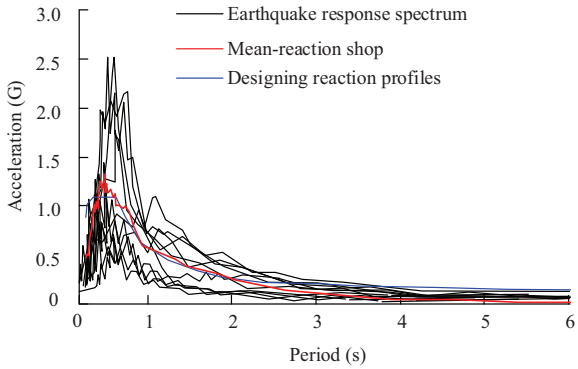

Fig. 6. Seismic response spectra of a 4-story multi ribbed composite plate structure

4.2. IDA Analysis of dense rib composite wall panel structures

By analyzing the seismic response of the above MRCW plate structure, the spacing of PGA ranges from 0.05 g to 0.05 g^{-1} g. Under 300 operating conditions, IDA analysis is conducted on the structure, as shown in Fig. 7.

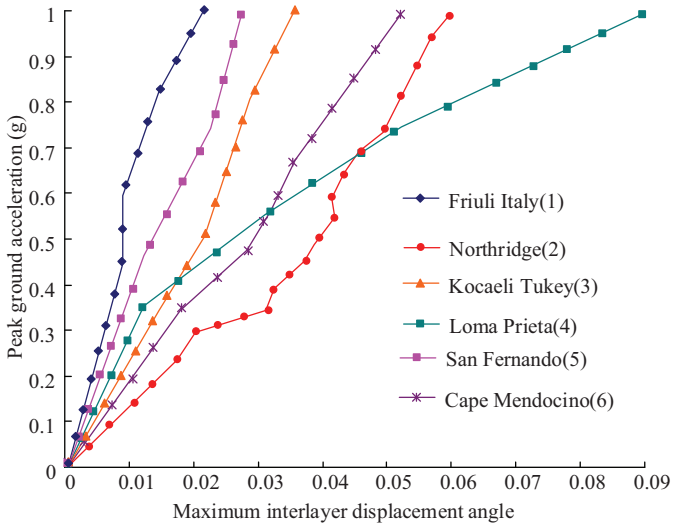

Fig. 7. IDA curve

Fig. 7 displays the IDA of the maximum DA of the structure under various working conditions. When the peak ground acceleration is 1.0 g, the maximum DA of the 4-story MRCW plate structure under the action of seismic wave No. 3 is 0.0861, and the minimum under the action of seismic wave No. 1 is 0.0196. The IDA calculation results are linearly regressed in logarithmic space to obtain the seismic probability demand model and parameters of the structure. The fitting results and vulnerability curve are shown in Fig. 8.

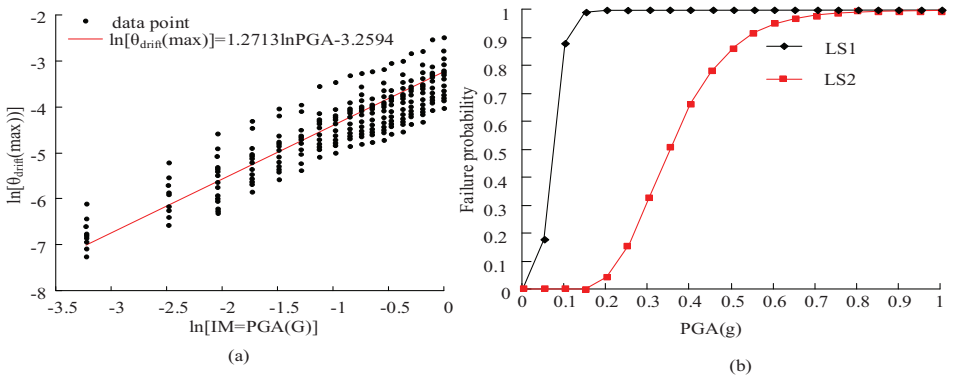

Fig. 8. Fitting results and vulnerability curve: a) Seismic demand modelling of 4-ply dense ribbed composite panel structures, b) Perishability Curve

In Fig. 8a shows the seismic demand model of a 4-story MRCW plate structure. According to the curve fitting results, as $\ln(IM)$ increases, the logarithmic value of the maximum displacement angle shows a stable upward trend. The value of parameter $\beta_{D/IM}$ is 0.4209. According to Technical Specification for Dense Ribbed Composite Plate Structure (JGJ/T275-2013), for dense ribbed composite plate structure, the horizontal displacement of the structure should be calculated, and the maximum interstorey displacement angle of the floors calculated according to the elasticity method of the structure under the action of multiple earthquakes should not be greater than the limit of elasticity displacement angle of the structure (1/800), and the limit of elastic-plasticity displacement angle of the floors is 1/100. Fig. 8b shows the vulnerability curve of a 4-layer multi ribbed composite plate structure at the above limit states. The LS1 displacement angle limit is 1/800. The LS2 displacement angle limit is 1/100. From the seismic vulnerability curve, the failure probability of LS1 in a 4-layer multi ribbed composite plate structure stabilizes at 1 after 0.20 g. The failure probability of LS2 enters a rapidly increasing stage after 0.20 g, and the failure probability is 1 after 0.80 g. The PGA corresponding to a 50% failure probability of the structure is the median value, which can be used to characterize the seismic performance of the structure.

4.3. Analysis of optimisation results for dense ribbed composite wall panel structures

At 0.35 g, the exceeding probability of LS2 for a 4-layer multi ribbed composite plate structure reaches 50% in the limit state. 0.35 g is used as the IM value for optimizing the design of a 4-layer structure. When the PGA is 0.35 g, the structure has the highest response under the action of seismic wave No. 2. Therefore, the seismic wave No. 2 is chosen as the input seismic motion for the optimization design of the 4-layer multi ribbed composite plate. The seismic peak acceleration is PGA = 0.35 g. The constrained SSO algorithm is used to optimize the seismic performance of 4-layer MRCW panels. Truncated normal

distribution is a random distribution of continuous design variables used for analysis. The upper and lower boundaries of the truncated normal distribution are taken as the upper and lower boundaries of the continuous design variable design domain. The standard deviation is taken as 1/3 of the distance from the center of the defined domain to the upper and lower boundaries. The number of samples per layer is $N = 50$. The maximum number of sampling layers is 50. The initial inter layer conditional probability is 0.2. The sampling process and the iterative results of the maximum inter story displacement angle are shown in Fig. 9.

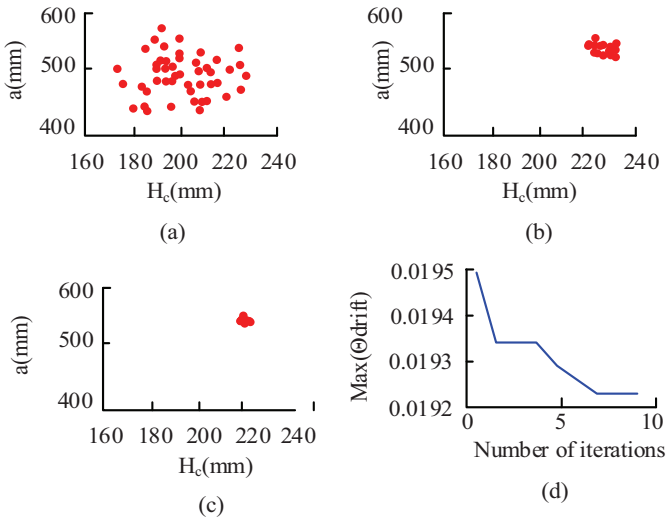

Fig. 9. Sampling process and maximum inter story displacement angle iteration results: a) First layer, b) Fifth floor, c) Ninth floor, d) Maximum angular cha interlayer displacement

In Fig. 9, With the change of iteration, the column section height and equivalent slant support brace width change from discrete distribution to aggregation. Finally, the sampling is stable in the 9th layer. At this time, the section height of the continuous column is 230 mm, and the equivalent width of the slant support is 525. Fig. 9d shows after 7 iterations, the maximum displacement angle stabilizes at 0.01922, The optimized structure of SSO algorithm performs IDA analysis. The vulnerability curve of the optimized 4-layer MRCW panel structure is shown in Fig. 10.

Fig. 10 displays the results of the vulnerability curves for the 4-layer MRCW panel structure before and after SSO algorithm optimization. By comparison, the failure probability of both extreme displacement angle states has decreased after optimization. Compared to LS1, LS2 has a more significant performance in reducing the failure probability. When PGA is 1.0 g, the optimized LS2 failure probability is less than 100%. When the PGA value is between 0.2 g and 0.6 g, the optimized LS1 and LS2 show a rapid upward trend as PGA increases.

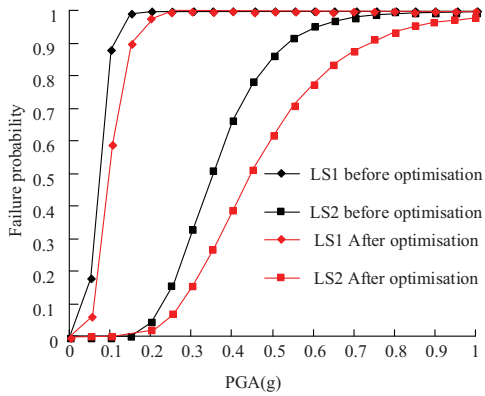

Fig. 10. Comparison of vulnerability curves

5. Conclusions

The study was conducted to optimise the wall structure of MRCW in order to make full use of its excellent structural performance in building construction. The constrained SSO algorithm is used to optimize the seismic performance of 4-layer MRCW panels. The results show that the section height and the equivalent slant support width of the continuous column for the 4-story multi ribbed composite wall panel change from discrete distribution to aggregation with the increase of iteration. Finally, the sampling is stable in the 9th layer. At this time, the section height of the continuous column is 230 mm, and the equivalent slant support width is 525.When PGA is 1.0 g, the optimized LS2 failure probability is less than 100%. When PGA values are between 0.2 g and 0.6 g, the optimized LS1 and LS2 show a rapid upward trend as PGA increases. This indicates that the constrained SSO algorithm has a good effect on the structural optimization of seismic performance for 4-layer multi ribbed composite wall panel structures. However, the research does not consider the effect of the wall panel and frame ratio on dynamic response. Further exploration of shape optimization is needed. At the same time, a linear restoring force model is used, which does not fully simulate the curve restoring force characteristics and multiple seismic responses. This is also an area that can be further improved in future research.

Acknowledgements

The research is supported by the general project of the “14th Five-Year Plan” of Liaoning Education Science in 2021: Construction of Professional Course System of Engineering Cost under Modern Apprenticeship (No. JG21BB108).

References

[1] S. Durdyev, S. R. Mohandes, S. Tokbolat, H. Sadeghi, and T. Zayed, “Examining the OHS of green building construction projects: a hybrid fuzzy-based approach”, *Journal of Cleaner Production*, vol. 338, pp. 590–602, 2022, doi: 10.1016/j.jclepro.2022.130590.

[2] Y.P. Liu, J.J. Li, W. Q. Chen, L.L. Song, and S.Q. Dai, "Quantifying urban mass gain and loss by a GIS-based material stocks and flows analysis", *Journal of Industrial Ecology*, vol. 26, no. 3, pp. 1051–1060, 2022, doi: 10.1111/jiec.13252.

[3] M. Tomczak and P. Jaskowski, "Harmonizing construction processes in repetitive construction projects with multiple buildings", *Automation in Construction*, vol. 139, pp. 266–288, 2022, doi: 10.1016/j.autcon.2022.104266.

[4] Q. Lin, S. C. Li, and Y.F. Zhu, "Analysis of hysteresis rule of energy-saving block and invisible multi-ribbed frame composite wall", *Structural Engineering and Mechanics*, vol. 77, no. 2, pp. 261–272, 2021, doi: 10.12989/sem.2021.77.2.261.

[5] J. Sun, L. Yuan, and P.F. Wang, "Residual bearing capacity of infilled frame of multi-ribbed composite wall after high temperature", *Construction and Building Materials*, vol. 214, pp. 196–206, 2019, doi: 10.1016/j.conbuildmat.2019.04.112.

[6] Z.A.B. Ismail, "Thermal comfort practices for precast concrete building construction projects: towards BIM and IOT integration", *Engineering Construction and Architectural Management*, vol. 29, no. 3, pp. 1504–1521, 2022, doi: 10.1108/ECAM-09-2020-0767.

[7] S. Han, Z. Lei, U. Hermann, A. Bouferguene, and M. Al-Hussein, "4D-based automation of heavy lift planning in industrial construction projects", *Canadian Journal of Civil Engineering*, vol. 48, no. 9, pp. 1115–1129, 2021, doi: 10.1139/cjce-2019-0825.

[8] M. Li, G.F. Jia, Z.B. Cheng, and Z. Shi, "Generative adversarial network guided topology optimization of doi: 10.1016/j.compstruct.2020.113254.

[9] H. Ezaldeen, S.K. Bisoy, R. Misra, and R. Alatrash, "Semantics-aware context-based learner modelling using normalized PSO for personalized e-learning", *Journal of Web Engineering*, vol. 21, no. 4, pp. 1187–1224, 2022, doi: 10.13052/jwe1540-9589.2148.

[10] L. Cao, W.Y. Zhang, X. Kan, and W. Yao, "A novel adaptive mutation PSO optimized SVM algorithm for sEMG-based gesture recognition", *Scientific Programming*, vol. 2021, pp. 823–836, 2021, doi: 10.1155/2021/9988823.

[11] G. Datola, M. Bottero, E. De Angelis, and F. Romagnoli, "Operationalising resilience: a methodological framework for assessing urban resilience through System Dynamics Model", *Ecological Modelling*, vol. 465, art. no. 109851, 2022, doi: 10.1016/j.ecolmodel.2021.109851.

[12] S. Oslund, C. Washington, A. So, T.T. Chen, and H. Ji, "Multiview robust adversarial stickers for arbitrary objects in the physical world", *Journal of Computational and Cognitive Engineering*, vol. 1, no. 4, pp. 152–158, 2022, doi: 10.47852/bonviewJCCE2202322.

[13] M. Ünver, M. Olgun, and E. Türkarslan, "Cosine and cotangent similarity measures based on Choquet integral for Spherical fuzzy sets and applications to pattern recognition", *Journal of Computational and Cognitive Engineering*, vol. 1, no. 1, pp. 21–31, 2022, doi: 10.47852/bonviewJCCE2022010105.

[14] D. Aikhuele, "Development of a statistical reliability-based model for data1, Revised: data2 the estimation and optimization of a spur gear system", *Journal of Computational and Cognitive Engineering*, vol. 2, no. 2, pp. 168–174, 2022, doi: 10.47852/bonviewJCCE2202153.

[15] P. Szeptyński and L. Mikulski, "Preliminary optimization technique in the design of steel girders according to Eurocode 3", *Archives of Civil Engineering,* vol. 69, no. 1, pp. 71–89, 2023, doi: 10.24425/ace.2023.144160.

Received: 2023-09-05, Revised: 2023-11-28